HHS Public Access

Author manuscript

Angew Chem Int Ed Engl. Author manuscript; available in PMC 2017 September 12.

Published in final edited form as:

Angew Chem Int Ed Engl. 2016 September 12; 55(38): 11387–11391. doi:10.1002/anie.201604014.

Accelerating Enzymatic Catalysis Using Vortex Fluidics

Joshua Britton[a,b], **Luz M. Meneghini**[c], **Colin L. Raston**[b], and **Gregory A. Weiss**[a,c]

[a]Mr. Joshua Britton and Professor Dr. Colin L. Raston, Chemical and Physical Sciences, Flinders University, Bedford Park, Adelaide, Australia, 5001

[b]Professor Dr. Gregory A. Weiss, Department of Chemistry, University of California, Irvine, Irvine, California, CA, 92697-2025, USA

[c]Ms. Luz M. Meneghini and Professor Dr. Gregory A. Weiss, Department of Molecular Biology and Biochemistry, University of California, Irvine, Irvine, California, CA, 92697-2025, USA

Abstract

Enzymes catalyze chemical transformations with outstanding stereo- and regio-specificities, but many enzymes are limited by their long reaction times. Here, we describe a general method to accelerate enzymes using pressure waves contained within thin films. Each enzyme responds best to specific frequencies of pressure waves, and we report acceleration landscapes for each protein. A vortex fluidic device introduces pressure waves that drive increased rate constants (k_{cat}) and enzymatic efficiency (k_{cat}/K_m). Four enzymes displayed an average seven-fold acceleration with deoxyribose-5-phosphate aldolase (DERA) achieving an average 15-fold enhancement through this approach. In solving a common problem in enzyme catalysis, we have uncovered a powerful, generalizable tool for enzyme acceleration. This research provides new insights into previously uncontrolled factors affecting enzyme function.

Graphical abstract

Enzymes – They're Picking Up Good Vibrations: A simple, generalizable approach to accelerate enzymes through the use of pressure waves in thin films has been developed. Each enzyme responds best to specific vibrations uncovering a previously unappreciated aspect of biocatalysis.

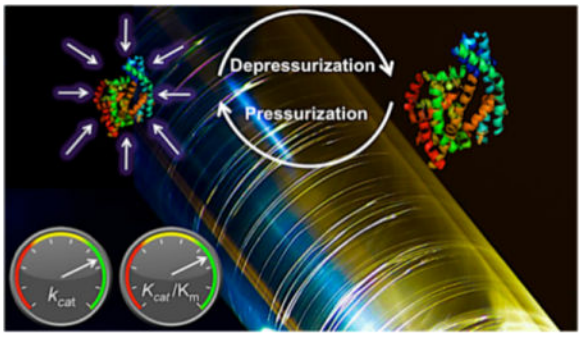

Correspondence to: Colin L. Raston; Gregory A. Weiss.

Supporting information for this article is given *via* a link at the end of the document.

Keywords

Biocatalysis; Enzyme acceleration; Aldolase; Hydrolases; Vortex Fluidics

Enzymes make life possible by catalyzing diverse and challenging chemical transformations with exquisite specificity. Applications in both industry[1] and academia[2] rely on the selectivity and power of enzymes to catalyze otherwise challenging transformations. Biocatalysts offer remarkable rate accelerations compared to uncatalyzed reactions, with typical rate accelerations (k_{cat}/k_{uncat}) of 10^5- to 10^{15}-fold faster.[3] Though some enzymes are diffusion-limited,[4] the catalytic rates of enzymes are often more typically limited by their catalytic efficiency (k_{cat}/K_m); additionally, molecular crowding, along with product and substrate inhibition, can reduce enzyme efficiency.[5] Though some enzymes catalyse transformations with rapid rates (e.g., laccases, fumarases and alcohol dehydrogenases),[6] other enzymes operate at only modest reaction rates, requiring long reaction times and carefully optimized conditions; for example, DERA requires long processing times (hours to days), and is substrate-inhibited.[7] We report a process that accelerates four different enzymes at standard temperature and pressure, but many water-soluble enzymes could be accelerated.

Recently, vortex fluidic devices (VFDs) have been used to accelerate covalent and non-covalent bond formation. VFDs process solutions in thin films by the rapid rotation of a sample tube (Figure 1).[8] Within the thin film, species are subjected to high levels of shear stress, mass transfer, and vibrational energy input at specific rotational speeds. For example, the VFD demonstrated the effective folding of four different proteins within minutes at standard temperature and pressure.[9] The VFD has also been used to improve the synthesis of lidocaine[10] and several other organic transformations.[11] In a continuous flow regime, flow rates of up to 20 mL/min can be achieved to process up to 30 L per day in the current, benchtop configuration. Since VFD processing increased the rates of organic reactions and protein folding, we hypothesized biocatalysis, which requires both reactivity and correct protein fold could benefit.

Control reactions with alkaline phosphatase demonstrated the requirements for high, specific rotational speeds of the VFD to generate a thin film containing the enzyme for accelerated catalysis (Figures S2, S3 and S4). VFD-mediated acceleration of four biocatalysts was compared to identical unprocessed enzyme-substrate solutions for efficient reaction optimization (Figure 2). First, VFD processing times were varied to identify short time periods (10 min to 2 h) suitable for further optimization (Figure 2A). Esterase produced a lower VFD-based enhancement (two-fold) compared to the other three enzymes; esterase also needed longer reactions times due to the enzyme's requirements for low substrate concentrations.[12] In general, after long time periods, the substrate is expended, and the unprocessed solution can attain similar levels of substrate conversion. Furthermore, VFD-processed solutions display parallel activities to the non-VFD counterparts for the first few minutes before rapid acceleration (e.g., alkaline phosphatase in Figure S9). A similar lag period before rate acceleration has been described previously for ultrasound-accelerated enzyme acceleration.[13]

Next, substrate and enzyme concentrations were simultaneously varied for the rapid scanning of reaction space to find effective reaction conditions (Figure 2B). This optimization unexpectedly revealed that VFD-mediated enzyme reactions are less susceptible to substrate inhibition than conventional conditions. For example, β-glucosidase without VFD processing encounters substrate inhibition at around 3.1 mM 4-nitrophenyl β-D-glucopyranoside; VFD processing delays the onset of substrate inhibition until almost a three-fold higher concentration (Figure S10B). With the exception of DERA, the three enzymes tolerated higher concentrations of substrate without losing VFD-mediated acceleration. This decrease in substrate inhibition suggests the VFD increases enzymatic k_{cat}, as further demonstrated below. DERA catalyzed the retro-aldol reaction of a pro-fluorophore at 144 μmol $h^{-1}L^{-1}$ when processed in the VFD (7.90 krpm rotational speed), compared to 10.7 μmol $h^{-1}L^{-1}$ under non-VFD conditions. DERA has previously been employed to synthesize high-value, complex, polyoxygenated compounds.[7b] The VFD-mediated DERA reaction achieved an average 15-fold enhancement. Conventional approaches to improving DERA have applied extensive screening[7b] and multiple rounds of error-prone PCR. For example, screening 20,000 colonies yielded a 10-fold increase in DERA activity.[14] Comparing the efforts required to achieve >10-fold acceleration by VFD in several days with conventional protein engineering, highlights the power of the approach reported here.

Enzyme acceleration by the VFD is sensitive to the tilt angle of the sample tube and the viscosity of the solution (Figure 2D–E). A tilt angle of 45° provided the strongest response, as has been previously observed in other VFD experiments.[8b] Second, concentrations of viscous, steric crowding reagents that decrease or terminate enzymatic catalysis in the non VFD-mediated control conditions were overcome in the VFD. Biocatalytic acceleration was achieved, for example, in high concentrations of PEG 8000 (6.00 mg/ml, 0.75 M), a condition that suppresses enzymatic catalysis in non-VFD conditions. Through rapid micro mixing or other associated phenomena, VFD-processed alkaline phosphatase tolerated high concentration of PEG 8000, resulting in ≈9-fold enhancement. The relative indifference to high concentrations of substrate and steric crowding suggests the VFD could be applied to processes requiring complex mixtures and minimal amounts of solvent.

The dependence on rotational speeds was also specific to each enzyme (Figure 2C and S11). Such requirements likely reflect differences in enzyme size, structure and dynamics. Esterase for example was highly dependent on a single rotational speed for enhanced activity. When processing esterase under VFD-mediated conditions, the only rotational speed to generate an enhancement was 8.00-krpm; at all other rotational speeds, the enzyme behaved similarly to non-VFD-mediated conditions. To map out the fine details of such resonances, a high-resolution scan of rotational speeds examined the acceleration of alkaline phosphatase and β-glucosidase (Figure 3). The rotational landscapes are intricate with little overlap of optimal rotational speeds. Device-specific variations in rotational landscapes were also observed, likely due to differences between device bearings and components (e.g., the Teflon collar, which wears due to friction from the sample tube); thus, Figure 3 depicts two enzymes processed by a single VFD. In addressing this issue of wear, and avoiding variable vibrations, we turned to 3D printing. Fabricating the collar out of high-density ABS plastic

allowed an interchangeable sleeve to be incorporated. Changing the insert upon wear insures reproducibility of the reported experiments (Figure S19).

Michaelis-Menten-based experiments were performed with β−glucosidase, and the kinetic constants for both VFD-processed and non-VFD conditions were derived (Table 1). The k_{cat} in the VFD-mediated reaction was around 2.5-fold faster than the non-VFD reaction (Figure 3). A lower Michaelis-Menten constant (K_m) was also obtained for the VFD-processed enzyme-substrate solution; 2.50 mM compared to 3.76 mM for a non-VFD mediated reaction. The decrease in K_m demonstrates the higher affinity for the β-glucosidase-substrate interaction under VFD-mediated conditions. The increase of k_{cat} and the decrease in K_m leads to an increase in enzyme efficiency (k_{cat}/K_m) of around 3.5-fold for the VFD-mediated reaction.

We hypothesize that enzymes are accelerated in the VFD from the instantaneous pressure changes generated by Faraday waves. Three possible mechanisms could harness such pressures. Firstly, transient pressurization of the active site around the substrate could occur. In this situation, a decrease in the active site volume through pressurization[15] could increase the turnover number of the enzyme; such enhancement follows from the Van't Hoff equation.[16] Secondly, pressure-induced protein conformational changes could occur at accelerated rates.[17] As enzymatic catalysis correlates with protein motion, faster protein motions could accelerate catalysis by contributing to the rate-determining process.[17] Thirdly, enzymatic catalysis requires a fine balance between protein stability and conformational flexibility.[18] Pressure-driven conformational changes may increase enzyme activity through β and α-relaxations.[19] These small changes can lead to the acquisition of protein conformations more suited for catalysis.[18]

The rotational landscape is specific for each enzyme studied, and appears to result from enzyme-specific preferences. Single-molecule experiments have elucidated the range of speeds and conformations required for enzymatic catalysis, which are specific for each enzyme.[20] The range of acceleration observed here falls within the expected range of enzyme speeds uncovered through such experiments. Thus, the VFD-driven rate acceleration could simply shift the distribution of enzyme conformational states to favor catalytic events. In future experiments, shaped Faraday waves with specific timing could provide further control and enhancement of biocatalysis.

In conclusion, we have demonstrated that the VFD effectively accelerates four enzymes, and establish a general, simple method to make biocatalysis more practical. VFD-mediated rate acceleration could find broad applicability in chemical transformations at industrial and laboratory scales.

Supplementary Material

Refer to Web version on PubMed Central for supplementary material.

Acknowledgments

JB thanks the Taihi Hong Memorial foundation and Kritika Mohan for photography. LM acknowledges the Miguel Velez Scholarship at UCI. GW gratefully acknowledges the National Institute of General Medical Sciences of the NIH (1RO1-GM100700-01). CR acknowledges the Australian Research Council and the Government of South Australia for their financial support during this project.

References

1. a) Aehle, W. Enzymes in Industry. WILEY-VCH; Weinheim: 2004. b) Nestl BM, Nebel BA, Hauer B. Curr Opin Chem Biol. 2011; 15:187–193. [PubMed: 21195018] c) DiCosimo R, McAuliffe J, Poulose AJ, Bohlmann G. Chem Soc Rev. 2013; 42:6437–6474. [PubMed: 23436023] d) Pollard DJ, Woodley JM. Trends Biotechnol. 2007; 25:66–73. [PubMed: 17184862] e) Choi JM, Han SS, Kim HS. Biotechnol Adv. 2015; 33:1443–1454. [PubMed: 25747291]
2. a) Renata H, Wang ZJ, Arnold FH. Angew Chem Int Edit. 2015; 54:3351–3367.b) Wang ZJ, Renata H, Peck NE, Farwell CC, Coelho PS, Arnold FH. Angew Chem Int Edit. 2014; 126:6928–6931.c) Siegel JB, Smith AL, Poust S, Wargacki AJ, Bar-Even A, Louw C, Shen BW, Eiben CB, Tran HM, Noor E, Gallaher JL, Bale J, Yoshikuni Y, Gelb MH, Keasling JD, Stoddard BL, Lidstrom ME, Baker D. P Natl Acad Sci USA. 2015; 112:3704–3709.d) Wallace S, Balskus EP. Angew Chem Int Edit. 2015; 54:7106–7109.e) Srivastava P, Yang H, Ellis-Guardiola K, Lewis JC. Nat Commun. 2015; 6
3. a) Bommarius, AS., Riebel, BR. Biocatalysis. Wiley-VCH; Weinheim: 2004. b) Koeller KM, Wong CH. Nature. 2001; 409:232–240. [PubMed: 11196651] c) Schramm VL. Annu Rev Biochem. 1998; 67:693–720. [PubMed: 9759501]
4. Stroppolo ME, Falconi M, Caccuri AM, Desideri A. CMLS, Cell Mol Life Sci. 2001; 58:1451–1460. [PubMed: 11693526]
5. Nelson, DL., Cox, MM. Lehninger Principles of Biochemistry. 5th. W H Freeman; New York: 2008.
6. Wolfenden R, Snider MJ. Accounts Chem Res. 2001; 34:938–945.
7. a) Subrizi F, Crucianelli M, Grossi V, Passacantando M, Botta G, Antiochia R, Saladino R. ACS Catalysis. 2014; 4:3059–3068.b) Greenberg WA, Varvak A, Hanson SR, Wong K, Huang H, Chen P, Burk MJ. P Natl Acad Sci USA. 2004; 101:5788–5793.
8. a) Britton J, Dalziel SB, Raston CL. Green Chem. 2016; 18:2193–2200.b) Britton J, Dalziel SB, Raston CL. RSC Adv. 2015; 5:1655–1660.
9. Yuan TZ, Ormonde CFG, Kudlacek ST, Kunche S, Smith JN, Brown WA, Pugliese KM, Olsen TJ, Iftikhar M, Raston CL, Weiss GA. ChemBioChem. 2015; 16:393–396. [PubMed: 25620679]
10. Britton J, Chalker JM, Raston CL. Chem Eur J. 2015; 21:10660–10665. [PubMed: 26095879]
11. a) Yasmin L, Chen X, Stubbs KA, Raston CL. Sci Rep. 2013; 3b) Britton J, Raston CL. RSC Adv. 2014; 4:49850–49854.c) Britton J, Raston CL. RSC Adv. 2015; 5:2276–2280.
12. Menger FM, Ladika M. J Am Chem Soc. 1987; 109:3145–3146.
13. Zhu K, Liu H, Han P, Wei P. Frontiers of Chemical Engineering in China. 2010; 4:367–371.
14. Jennewein S, Schürmann M, Wolberg M, Hilker I, Luiten R, Wubbolts M, Mink D. Biotechnology Journal. 2006; 1:537–548. [PubMed: 16892289]
15. Hillson N, Onuchic JN, García AE. P Natl Acad Sci USA. 1999; 96:14848–14853.
16. Kuster, CJT., Scheeren, HW. In High Pressure Chemistry. Wiley-VCH; Weinheim: 2007.
17. Hay S, Scrutton NS. Nat Chem. 2012; 4:161–168. [PubMed: 22354429]
18. Henzler-Wildman KA, Lei M, Thai V, Kerns SJ, Karplus M, Kern D. Nature. 2007; 450:913–916. [PubMed: 18026087]
19. Shrestha UR, Bhowmik D, Copley JRD, Tyagi M, Leão JB, Chu X-Q. P Natl Acad Sci USA. 2015; 112:13886–13891.
20. a) Sims PC, Moody IS, Choi Y, Dong C, Iftikhar M, Corso BL, Gul OT, Collins PG, Weiss GA. J Am Chem Soc. 2013; 135:7861–7868. [PubMed: 23631749] b) Xie S. Single Mol. 2001; 2:229–236.

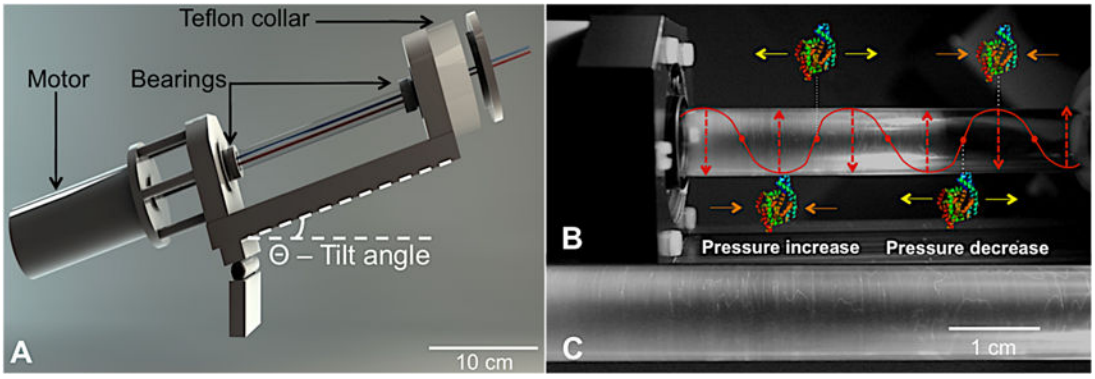

Figure 1.

The VFD and its Faraday waves. **(A)** A schematic of the VFD. **(B)** A VFD sample tube containing 5 mL solution rotating at 3.50 krpm at a tilt angle, θ, of 45°, shows Faraday waves formed within the thin film. Overlaid schematically, such pressure waves can affect the enzyme-substrate complex. **(C)** This enlargement focuses on VFD-generated Faraday waves. Additional images of Faraday waves can be found in Figure S14.

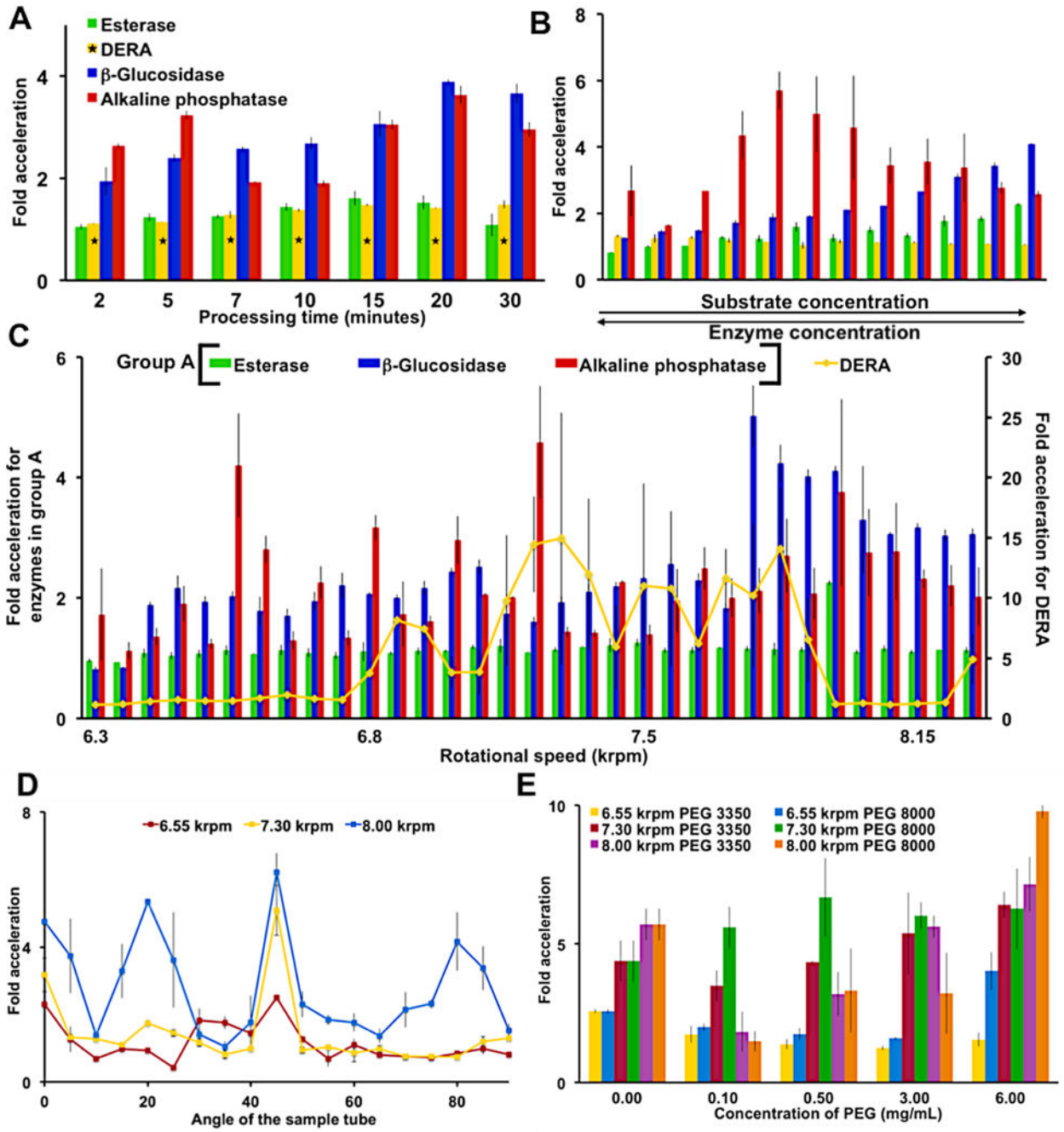

Figure 2.

Parameters for accelerated biocatalysis of the four enzymes. Fold acceleration was determined by the ratio of the VFD-mediated substrate conversion to an identical enzyme-substrate solution not treated by the VFD. **(A)** A time dependent study at a fixed rotational speed (8.00 krpm) reveals processing times for further optimization. As indicated with a DERA required longer reaction times of 60, 80, 100, 120, 140, 160 and 180 min. **(B)** Simultaneous changes to the substrate and enzyme concentrations at a 8.00 krpm rotational speed mapped the reaction landscape (Table S2A–D). **(C)** Rotational speed scans in 50 rpm

increments identify harmonic oscillations associated with Faraday wave-promoted biocatalysis. Error bars are larger for DERA than any other enzyme due to the product's non-linear, fluorescence calibration curve. **(D)** Varying the tilt angle of the sample tube identifies 45° as optimal. Thus, a 45° tilt angle was used throughout this report. **(E)** The addition of PEG dramatically slowed the non-VFD control, but the VFD processed solution demonstrated significant catalytic activity. Error bars indicate the standard deviation around the mean (n=3 with three independent measurements on three different VFDs). With the exception of a single data point requiring 90% confidence limits, all data reported here have no overlapping errors within 95% confidence limits. The concentrations of enzymes and substrates are as follows: alkaline phosphatase (6.77 nM) and its substrate *p*-nitrophenol phosphate (0.17 mM), β-glucosidase (19.3 nM) and its substrate 4-nitrophenyl β-D-glucopyranoside (7.5 mM), esterase (0.12 nM) and its substrate p-nitrophenol acetate (44 μM) and DERA (7.69 μM) and its fluorogenic substrate (0.52 mM) unless otherwise indicated, and as described in Table S2A-D.

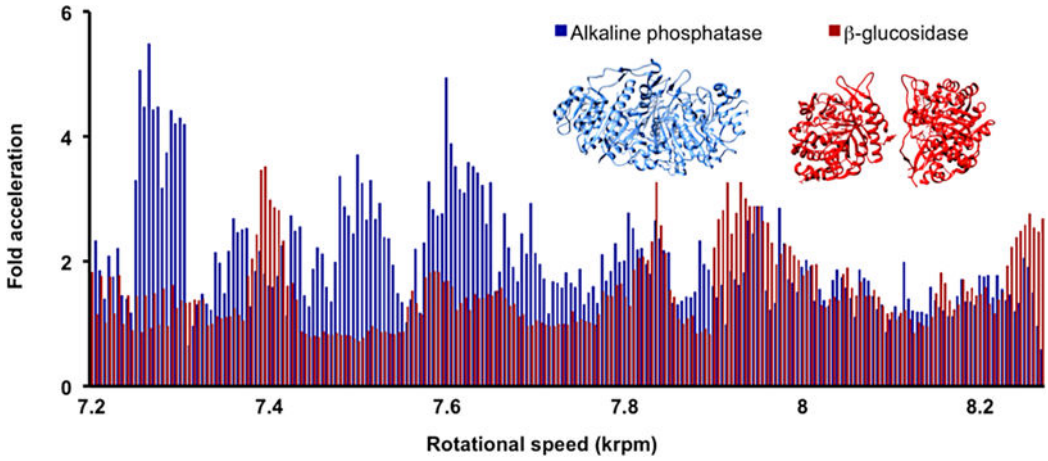

Figure 3.

The rotational landscape of β-glucosidase and alkaline phosphatase. Though the two enzymes have similar levels of response at some rotational speeds, distinctly different rotational landscapes are revealed. The results demonstrate the enzyme specificity of VFD-mediated acceleration. Each data point represents the mean (n=2) for a 10 min reaction at the indicated rotational speeds. The alkaline phosphatase enzyme-substrate solution used Fast alkaline phosphatase (6.77 nM) and *p*-nitrophenol phosphate solution (0.17 mM) whilst the β−glucosidase enzyme-substrate system used β-glucosidase (19.3 nM) and 4-nitrophenyl β-D-glucopyranoside (7.5 mM).

Table 1

Michaelis-Menten parameters for the VFD *vs.* non-VFD mediated processing of β-glucosidase.*

Parameter	Non VFD-mediated reaction	VFD-mediated rate acceleration
V_{max} (nM s^{-1})	128 ± 5.71	309 ± 52.4
K_m (mM)	3.76 ± 0.15	2.50 ± 0.44
k_{cat} (s^{-1})	13.4 ± 0.59	32.1 ± 5.45
k_{cat}/K_m ($mM^{-1}s^{-1}$)	3.55 ± 0.19	13.32 ± 4.03

* For this VFD-process, β-glucosidase (9.26 nM), a rotational speed of 7.60 krpm was used, as this provided the most consistent enhancement over sustained time periods. Error indicates the standard deviation around the mean (n=3). There was no overlapping error at 95% confidence limits. The raw data was fitted to a Michaelis-Menten plot and analyzed using a least squares fitting (LSF) approach (Figures S17 and S17).